

ANISOTROPIC Ag CONTRIBUTION TO TRANSPORT PHENOMENA IN Ag-Bi₂Sr₂CaCu₂O_y BULK CRYSTAL

Manabu IKEBE, Hiroyuki FUJISHIRO and Koshichi NOTO

Department of Materials Science and Technology, Faculty of Engineering,
Iwate University, 4-3-5 Ueda, Morioka 020-8551, Japan.

Anisotropies in the electrical resistivity are studied on Ag-doped Bi₂Sr₂CaCu₂O_y (Bi2212) bulk crystals prepared by the floating zone method. Anisotropic Ag contributions to the resistivity are analyzed based on a proposed generalized circuit model. Possible correlation between Ag compensation for the weak-links and the anisotropic Ag contribution to the resistivity is suggested. Dynamic stability as a superconducting material is also discussed.

1. INTRODUCTION

Recently, high T_c bulk oxide superconductors have come to be used for practical application such as the power leads for a superconducting magnet. The very small thermal conductivity which prevents heat intrusion into the cryogenic system is a merit of oxides in addition to the intrinsic high transition temperature T_c. There are many reports on the critical current (J_c) enhancement caused by Ag-doping in bulk ceramic samples which is believed to come from improvement of the weak links between grain boundaries. In case that the weak links limit the supercurrent, it is possible that the observable critical current is not intrinsic critical current J_c but rather is the quench current J_q¹ which is smaller than J_c. J_q is closely related to the dynamic stability of superconductors through the concept of the minimum propagating zone l_{MPZ} ² which is defined as

$$l_{MPZ} = \sqrt{\frac{2\kappa(T_c - T_0)}{J^2\rho}}, \quad (1)$$

where J is the electric current, ρ and κ are the normal state electrical resistivity and thermal conductivity near T_c, and T₀ is the background temperature of the current

carrying superconductor. l_{MPZ} is obtained by balancing generating joule heat in a thermally activated normal zone with outgoing heat from the normal zone. Under the flow of the current J , the normal zone larger than l_{MPZ} will grow because heat generation exceeds cooling. Thus the normal state electrical resistivity and thermal conductivity are important parameters to determine the dynamic stability of superconductors.

Previously, Kubo et al. of Japan Fine Ceramics Center (JFCC) reported the preparation of high J_c Bi2212 bulk crystals by floating zone (FZ) method³ and the effects of Ag-doping on J_c characteristics were also investigated.⁴ The addition of Ag enhanced the thermal conductivity^{5,6} and should also enhance the electrical conduction, improving the dynamic stability. In this paper, we measured anisotropic electrical transports of Ag-doped FZ-Bi2212 crystals and analyzed the anisotropic Ag contribution. The anisotropic thermal conductivities were estimated using the anisotropy ratio of Ag contribution calculated from the electrical resistivity.

2. EXPERIMENTAL PROCEDURE

FZ-Bi2212 bulk crystals with 0, 10 and 15wt.% Ag were prepared at JFCC. The samples were cut into rectangular bars with typical sizes $6 \times 2 \times 2 \text{ mm}^3$. The largest edge was along the direction of the crystal growth (G-direction) which was parallel to the crystallographic ab-plane. The c-axis was assumed to be perpendicular to this plane. We call this assumed axis as C*-direction. We also denominate the remaining direction (perpendicular to both G-direction and C*-direction) as P-direction. The electrical resistivity was measured by a standard four-terminal method above 78K.

3. EXPERIMENTAL RESULTS

Figure 1(a) shows the temperature dependences of the electrical resistivities in G-direction of Bi2212 crystals doped by 10wt.%Ag (ρ_G^{10} for sample #10A), 15wt.%Ag (ρ_G^{15} for sample #15A) and without Ag doping (ρ_G^{00} for sample #00A). We notice that all specimens show superconducting transition at about 80K. Figure 1(b) shows the resistivities ρ_{C^*} vs. T in C*-direction and Fig. 1(c) shows the similar plots for ρ_P in P-direction. Figure 2 shows the anisotropy ratios ρ_P/ρ_G and ρ_{C^*}/ρ_G as a function of temperature for respective samples. The anisotropy ratio $\rho_{C^*}^{00}/\rho_G^{00}$ of the non-doped sample exceeds 200 over the whole temperature range. However, ρ_C/ρ_{ab} of good single

crystals is known to take a value approximately $10^{4.7}$. It is also noticed that the anisotropy ratio ρ_p^{00}/ρ_G^{00} is also large exceeding 30. The not so large $\rho_{C^*}^{00}/\rho_G^{00}$ may reflect the incomplete alignment of the c-axis of each grain in the present crystal. We can see that the anisotropy ratio, ρ_{C^*}/ρ_G is remarkably reduced in Ag-doped samples, while the corresponding reduction in the ratio ρ_p/ρ_G is moderate.

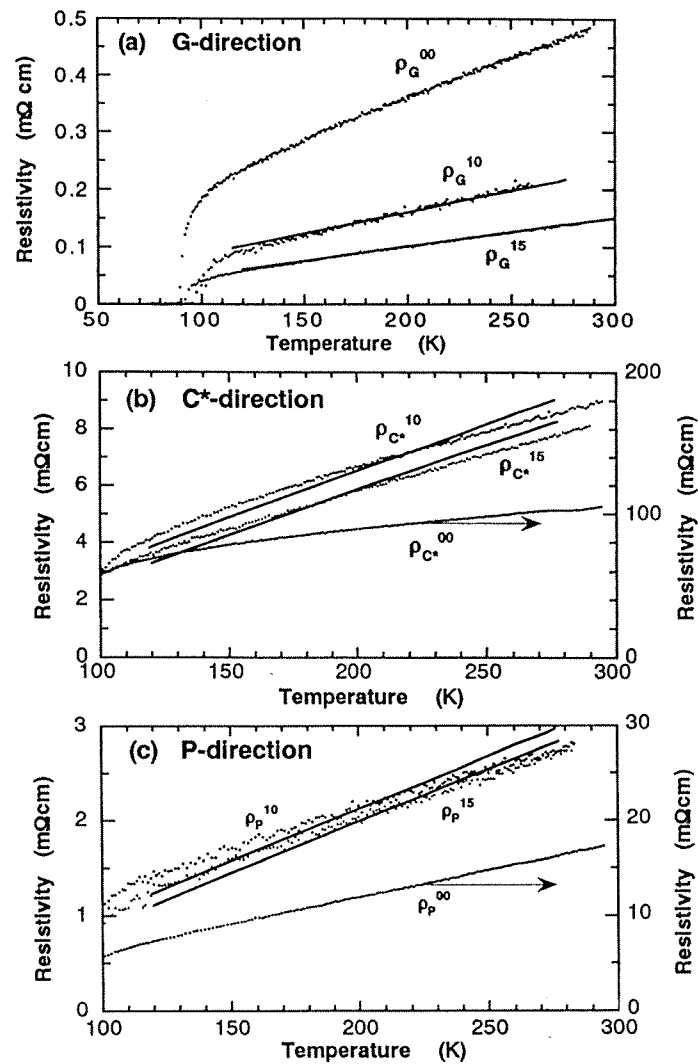


FIGURE 1. Temperature dependences of the (a) G-direction, (b) C*-direction and (c) P-direction, electrical resistivity of Bi2212 crystals doped by 0wt.% (ρ^{00}), 10wt.% (ρ^{10}) and 15wt.% (ρ^{15}) Ag. Calculated electrical resistivity curves are also shown.

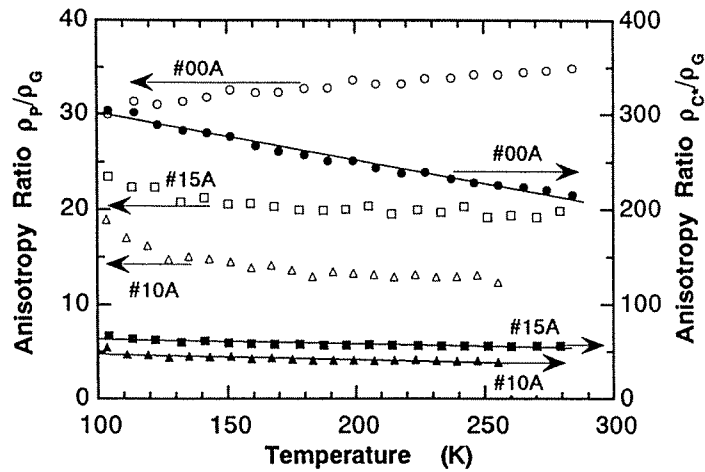


FIGURE 2. Temperature dependence of the anisotropy ratios ρ_p/ρ_G and ρ_c/ρ_G for #00A (\circ, \bullet), #10A ($\triangle, \blacktriangle$) and #15A (\square, \blacksquare).

4. DISCUSSION

The resistivity of the Ag-Bi2212 composite should depend on the amount and the shape of the doped Ag particles, their orientations, the distributions and the probabilities to form mutual connections in the Bi2212 matrix. Figure 3 shows an example of the Ag distribution image by an electron probe microanalyzer (EPMA). We notice that the majority of Ag particles take elongated shapes nearly parallel to G-direction; Ag particle contribution to the transport phenomena should be very anisotropic. Some Ag particles are spherical or are elongated not parallel to G-direction.

For the analyses of anisotropic Ag contribution to the electrical resistivity, we propose a phenomenological model. The contribution of doped Ag particles can be approximated by a generalized electric circuit in Fig. 4(a), which consists of a combination of parallel and series electric paths of Ag and Bi2212. Then we simulate the generalized circuit visually by a model cube shown in Fig. 4(b), where the Ag paths along the pillars located at the cube sides stand for the parallel Ag resistance R_{Ag1} in Fig. 4(a) and the inside smaller Ag cube stands for the series resistance R_{Ag2} . The pillar thicknesses are assumed to depend on the direction of the specimen to allow for the anisotropic Ag contribution. We postulate that the inner cube corresponds mainly to the contribution of relatively isolated Ag particles inside the grains and the side pillars

reflect the contribution of nearly connected Ag particles located at the boundaries, though the strict separation of "isolated" and "connected" Ag particles might be difficult because Bi2212 matrix is also electrically conductive. The sum of the volume of the cube and side pillars is taken to be equal to the volume of doped Ag particles. It should

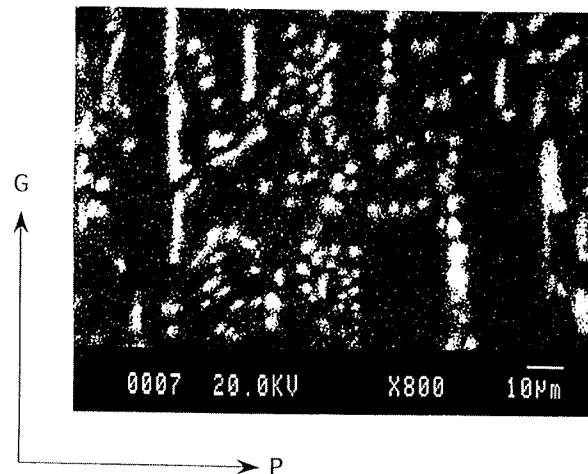


FIGURE 3. EPMA characteristic X-ray image of Ag at the surface of the 10wt.% Ag-doped specimen. G and P indicate the crystal growth direction (G) and perpendicular direction (P). C^* -direction is normal to the photograph.

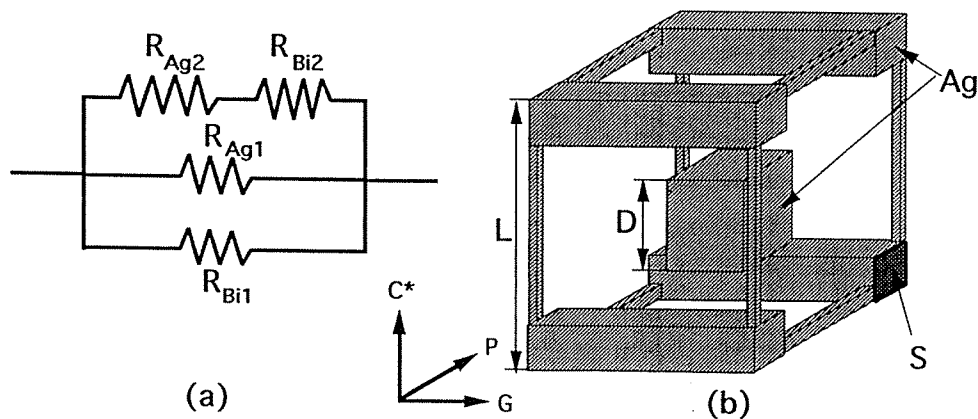


FIGURE 4. (a) An equivalent electric circuit of the Ag-Bi2212 composite material used in the analyses. (b) A phenomenological "anisotropic" model cube which classifies the doped Ag particles into "parallel Ag paths" (side pillars) and "series Ag path" (inner cube) based on the equivalent electric circuit.

be noticed that the conventional percolation theory cannot be applied to the present anisotropic and non-random case.

Next, we try to reproduce the observed temperature dependence of the electrical resistivity based on the model by adjusting the cross section of the Ag pillars and the size of the inner Ag cube. The total resistance R of the circuit in Fig. 4(a) is given by

$$\frac{1}{R} = \frac{1}{R_{Ag2} + R_{Bi2}} + \frac{1}{R_{Ag1}} + \frac{1}{R_{Bi1}}. \quad (2)$$

If the side length of the model cube is L , that of the inner cube D and the cross section of the pillar S , each resistance component is approximated as $R_{Ag2} = \rho_{Ag} D/D^2$, $R_{Bi2} = \rho_{Bi} (L-D)/D^2$, $R_{Ag1} = \rho_{Ag} L/(4S)$ and $R_{Bi1} = \rho_{Bi} L/(L^2 - D^2 - 4S)$ with ρ_{Ag} and ρ_{Bi} being the resistivities of Ag and Bi2212, respectively. We used $\rho(T)$ of undoped FZ-Bi2212 in Fig. 1 for $\rho_{Bi}(T)$ and that of Ag+0.085at.% Au alloy (residual resistivity ratio: RRR=37)⁸ for $\rho_{Ag}(T)$ because RRR is close to the estimated values of Ag particles in Bi2212 from the analyses of the thermal conductivity.⁵ The results of the fitting above 100K are shown in Figs. 1(a), (b) and (c) for G-, C*- and P-directions, respectively. The determined values of the several sizes of the model cube are summarized in Table I. We notice that the cross section of the Ag side pillars of the model cube critically depends on the directions, demonstrating very anisotropic Ag contributions as anticipated. The pillar cross section ratio along G-

Table I. Determined values of the several sizes of the model.

(1) Cross section of Ag side pillars S for $L=1$ and their ratios relative to G-direction.

	(#10A)		(#15A)	
	cross section S	ratio	cross section S	ratio
G-	8.1×10^{-4}	1.0	1.7×10^{-3}	1.0
C*-	4.1×10^{-5}	0.05	4.1×10^{-5}	0.02
P-	1.1×10^{-4}	0.13	9.8×10^{-5}	0.06

(2) Side length D of the inside Ag cube for $L=1$ and the ratio of the total volume of the side pillars to that of the inside cube.

	(#10A)	(#15A)
	D	0.40
ratio	0.0150	0.0189

C*- and P-directions is 1:0.05:0.13 for #10A and 1:0.02:0.06 for #15A. We expect that the proposed phenomenological model for anisotropic conduction is useful in some cases to promote our empirical understandings for the transport phenomena of composite materials.

As we have measured the electrical resistivity ρ_G and the thermal conductivity κ_G ⁵ in G-direction, we can estimate the minimum propagating zone l_{MPZ} in this direction. The ab-plane optimum $J_c=5360A/cm^2$ at 77K was attained for #10A, while J_c of #00A sample was 2900A/cm². Further increase of Ag-doping above 10wt.% degraded J_c values.⁴ l_{MPZ} at $T_0=77K$ is estimated to be 1.6mm for #00A and 2.5mm for #10A by the use of eq. (1). The dynamic stability is improved in #10A in spite of the enhanced J_c values. If we assume that the measured critical currents are really the quench currents J_q due to weak links, the weak links which cause the normal conducting region approximately of the same size as respective l_{MPZ} may be responsible for the quenching of each FZ-Bi2212 sample.

Finally we make a brief comment on the thermal conductivity κ . We reported the κ in G-direction (κ_G) of these FZ-Bi2212 samples⁵ and pointed out remarkable contributions of doped Ag particles as heat paths. We could not, however, measure κ_C and κ_P because of the limited sample dimension. Very anisotropic Ag contribution to ρ suggests that Ag contribution to κ should also be very anisotropic. If we assume that the ratio of anisotropic Ag contribution is the same for both transport phenomena, κ_G/κ_C is expected to increase by Ag-doping because the anisotropic ratio of the thermal conductivity, κ_{ab}/κ_c , of the single crystal Bi2212 ($\approx 6-8$)⁷ is rather smaller than the anisotropic contribution ratio of Ag. The anisotropy of κ must be taken into account in connection with the dynamic stability problem when Ag-doped FZ-Bi2212 is immersed in a coolant.

5. SUMMARY

Anisotropic Ag contributions to the electrical resistivity were examined and analyzed for Ag-doped $Bi_2Sr_2CaCu_2O_y$ prepared by FZ method. The Ag contributions were confirmed to be anisotropic not only between in the crystal growth direction (G-direction) and the oriented c-axis (C*-direction) but also between in C*-direction and the perpendicular direction (P-direction) in the ab-plane. The dynamic stability was found to be enhanced by 10wt.% Ag doping from the analyses of the minimum propagating zone.

ACKNOWLEDGEMENT

The authors wish to thank Y. Kubo and K. Michishita of Japan Fine Ceramics Center (JFCC) in the offer of the Ag-Bi2212 samples.

REFERENCES

- 1) M. Matsukawa, K. Noto, M. Ikebe, Y. Kashiwazaki, N. Matsuura, K. Watanabe and K. Mori, *Physica C* **185-189** (1991) 2477.
- 2) See, for example, Wilson, M.N., *Superconducting Magnet* (Clarendon Press, Oxford, (1983))
- 3) Y. Kubo, K. Michishita, Y. Higashida, H. Yokoyama, Y. Hayami, E. Inukai, A. Saji, N. Kuroda and H. Yoshida, *Jpn. J. Appl. Phys.* **28** (1989) L606.
- 4) Y. Kubo, K. Michishita, K. Shimizu, Y. Higashida, H. Yokoyama, Y. Hayami, E. Inukai, A. Saji, N. Kuroda and H. Yoshida, *Jpn. J. Appl. Phys.* **28** (1989) L1936.
- 5) M. Ikebe, H. Fujishiro, M. Matsukawa, F. Tatzaki, H. Ogasawara, K. Noto, K. Michishita and Y. Kubo, *Jpn. J. Appl. Phys.* **33** (1994) 2004.
- 6) M. Matsukawa, F. Tatzaki, K. Noto, H. Fujishiro, K. Michishita and Y. Kubo, *Cryogenics* **34** (1994) 685.
- 7) M.F. Crommie and A. Zettle, *Phys. Rev. B* **43** (1991) 408.
- 8) H. Fujishiro, M. Ikebe, T. Sasaoka and K. Nomura, *Cryogenics* **33** (1993) 1086.